

SAND99-2736J

Abstract Number: 545

Program Number: SS1+EM-TuA10

Deposition and characterization of highly oriented $Mg_3(VO_4)_2$ thin film catalysts

Judith A. Ruffner, Allen G. Sault, Mark M. Rodriguez, and Ralph G. Tissot, Jr.

Sandia National Laboratories, P. O. Box 5800, Mailstop 1349, Albuquerque, New Mexico

87185-1349

RECEIVED
OCT 28 1999
OSTI

Abstract

Magnesium vanadates are potentially important catalytic materials for the conversion of alkanes to alkenes *via* oxidative dehydrogenation. However, little is known about the active sites at which the catalytic reactions take place. It may be possible to obtain a significant increase in the catalytic efficiency if the effects of certain material properties on the surface reactions could be quantified and optimized through the use of appropriate preparation techniques. Given that surface reactivity is often dependent upon surface structure and that the atomic level structure of the active sites in these catalysts is virtually unknown, we desire thin film samples consisting of a single magnesium vanadate phase and a well defined crystallographic orientation in order to reduce complexity and simplify the study of active sites. We report on the use of reactive RF sputter deposition to fabricate very highly oriented, stoichiometric $Mg_3(VO_4)_2$ thin films for use in these surface analysis studies. Deposition of samples onto amorphous substrates resulted in very poor crystallinity. However, deposition of $Mg_3(VO_4)_2$ onto well-oriented, lattice-matched thin film "seed" layers such as Ti (0001), Au (111), or Pt (111) resulted in very strong

DISCLAIMER

This report was prepared as an account of work sponsored by an agency of the United States Government. Neither the United States Government nor any agency thereof, nor any of their employees, make any warranty, express or implied, or assumes any legal liability or responsibility for the accuracy, completeness, or usefulness of any information, apparatus, product, or process disclosed, or represents that its use would not infringe privately owned rights. Reference herein to any specific commercial product, process, or service by trade name, trademark, manufacturer, or otherwise does not necessarily constitute or imply its endorsement, recommendation, or favoring by the United States Government or any agency thereof. The views and opinions of authors expressed herein do not necessarily state or reflect those of the United States Government or any agency thereof.

DISCLAIMER

Portions of this document may be illegible in electronic image products. Images are produced from the best available original document.

preferential (042) crystallographic orientation (pseudo-hexagonal oxygen planes parallel to the substrate). This strong preferential growth of the $Mg_3(VO_4)_2$ suggests epitaxial (single-crystal) growth of this mixed metal oxide on the underlying metal seed layer. The effects of the seed layer material, deposition temperature, and post-deposition reactive treatments on thin film properties such as stoichiometry, crystallographic orientation, and chemical interactions will be discussed.

Sandia is a multiprogram laboratory operated by Sandia Corporation, a Lockheed Martin Company, for the United States Department of Energy under Contract DE-AC04-94AL85000.

Introduction

Although magnesium vanadates are potentially important catalytic materials for the conversion of alkanes to alkenes *via* oxidative dehydrogenation [1, 2, 3], little is known about the active sites at which the catalytic reactions take place. Most studies to date have been conducted on powdered magnesium vanadate samples that consist of randomly oriented crystallites, and which may contain multiple crystalline phases and have irregular surface structures. The orientation, phase, and surface structure of the constituent crystallites all affect the surface reactivity, making it difficult to isolate the effect of any one feature on surface reactivity. In order to simplify the study of the magnesium vanadate surface reactivity, we require thin film samples that consist of a single magnesium vanadate phase and a well defined crystallographic orientation. Furthermore, it is desirable that the films be extremely thin (i.e., < 10 nm) and deposited on an electrically conducting substrate in order to eliminate charging effects during application of ultra high vacuum (UHV) surface analysis. A similar arrangement has even allowed for analysis of ultra-

thin alumina films by scanning tunneling microscopy [4, 5]. Growth of such $\text{Mg}_3(\text{VO}_4)_2$ films will reduce the complexity of the surface structure and greatly simplify the study of active sites in these important materials.

Magnesium orthovanadate, $\text{Mg}_3(\text{VO}_4)_2$, was chosen as the target phase for synthesis due to a clear epitaxial relationship between the $\text{Mg}_3(\text{VO}_4)_2$ structure and the structure of several easily grown, well-oriented substrate materials. $\text{Mg}_3(\text{VO}_4)_2$ occurs in both a cubic [6] and an orthorhombic crystalline phase [7], but the orthorhombic phase is generally observed following preparation of $\text{Mg}_3(\text{VO}_4)_2$ catalysts by calcining a 3:1 mixture of MgO and V_2O_5 in air [8]. Furthermore, this phase has been shown to be active in the oxidative dehydrogenation of propane [1,8]. Krishnamachari and Calvo have reported that the orthorhombic $\text{Mg}_3(\text{VO}_4)_2$ structure is based upon a pseudo-cubic structure of hexagonal close packed (hcp) layers of oxygen atoms [9]. The pseudo-hcp planes comprise the (042) set of crystalline planes which are separated by a d-spacing of 2.3559 Å. The average spacing between oxygen atoms within the pseudo-hcp net is 2.96 Å. Based on this structure, several materials were selected as potential seed layer materials on which to initiate epitaxial growth of $\text{Mg}_3(\text{VO}_4)_2$ oriented with the (042) plane parallel to the substrate. The candidate seed layer materials were selected for their hexagonal close packed geometry [either fcc (111) or hcp (0001)], strong preferential growth in that orientation, and minimal reactivity with $\text{Mg}_3(\text{VO}_4)_2$ at temperatures of up to 500 °C. The resultant candidates are listed in Table I, along with their crystal structures, metal-metal spacing in the hcp planes, and relative lattice mismatch with the hcp (042) plane of oxygen in $\text{Mg}_3(\text{VO}_4)_2$. Although the seed layer materials generally exhibit strong preferential orientation with the hcp planes parallel to the plane of the substrate, their crystallites are probably randomly oriented within the plane of the

substrate. In other words, the grains in the metal films are aligned with the hcp planes parallel to the substrate but are rotated in plane with respect to one another. This strong preferential orientation in one direction only gives rise to a "fiber" texture in the films.

Experiment

Several $\text{Mg}_3(\text{VO}_4)_2$ thin films were deposited using RF reactive sputtering from stoichiometric ceramic targets. The films were deposited in a Unifilm PVD-300 Multisource Sputter System that allows sequential deposition from up to 5 sputter targets. This was especially useful in minimizing the lag time between deposition of a seed layer and the overlying $\text{Mg}_3(\text{VO}_4)_2$ film. By minimizing the lag time, we hoped to minimize contaminants on the pristine seed layer, thereby promoting epitaxial growth of the $\text{Mg}_3(\text{VO}_4)_2$ thin film deposited directly onto the crystalline seed layer. The base pressure of the system is $\sim 2.0 \times 10^{-7}$ Torr which results in deposition of a monolayer of residual gas contaminants on a pristine surface approximately every 5 seconds. All thin films were deposited using a chamber pressure of 10 mTorr. The source-to-substrate distance was 3.6 cm.

$\text{Mg}_3(\text{VO}_4)_2$ thin film samples were deposited onto oxidized Si wafers with and without seed layers to determine if preferential orientation could be forced. Si wafers were used as the substrates for Pt, Ag and Ti, while oxidized Si wafers were used as the substrates for Au because it reacted with the surfaces of non-oxidized Si wafers to form a silicide upon heating above 300°C. Seed layers, including Ti, Ag, Au, and Pt, were first deposited as single films onto oxidized Si wafers using the parameters listed in Table II. Standard θ -2 θ x-ray diffraction (XRD) analysis was then performed to determine the crystalline orientation of the resultant seed

layers. Seed layers that exhibited the preferred hexagonal close-packed orientation then were reproduced under identical conditions and coated immediately with an overlying thin film of $\text{Mg}_3(\text{VO}_4)_2$ without breaking vacuum.

$\text{Mg}_3(\text{VO}_4)_2$ thin films were deposited at temperatures of ~ 100 °C (ambient) and 300 °C in order to determine the effects of deposition temperature on the resultant crystalline structure. XRD was performed on these samples in order to assess crystallinity. In addition, the $\text{Mg}_3(\text{VO}_4)_2$ thin films were deposited in a reactive oxygen environment in order to ensure full oxidation of the thin films.

The bulk stoichiometry of the $\text{Mg}_3(\text{VO}_4)_2$ films was characterized using atomic absorption spectroscopy (AAS), while the surface stoichiometry was characterized using x-ray photoelectron spectroscopy (XPS). Samples were prepared for AAS by dissolving the $\text{Mg}_3(\text{VO}_4)_2$ film in concentrated HCl, and then diluting the resulting solutions prior to analysis on a Perkin Elmer 5100 PC instrument. XPS was performed using a VG Microtech Clam 2 operated at an analyzer resolution of 1.0 eV, with excitation provided by a VG Microtech XR3 Al $K\alpha$ X-ray source. The XPS system is housed in a UHV chamber coupled to an atmospheric reactor, which allows treatment of the films in reactive environments typical of those found during oxidative dehydrogenation, followed by transfer to UHV without intervening exposure to air. Quantitation of the XPS results was performed using published sensitivity factors [10] and integrated areas under the Mg 2s, Mg 2p, and V 3p XPS peaks. These peaks were chosen rather than the more intense Mg 1s and V 2p peaks since these latter photoelectrons (particularly the Mg 1s peak) have relatively short inelastic mean free paths (IMFP), and are therefore subject to

severe attenuation by carbonaceous overlayers often formed during reaction in hydrocarbon containing mixtures. The Mg 2s, Mg 2p, and V 3p photoelectrons all have relatively long IMFPs and are therefore less susceptible to attenuation. Furthermore, these photoelectrons all have very similar kinetic energies, so that any attenuation that does occur is of similar magnitude for all of the peaks, and the relative areas of the peaks are unaffected.

The crystalline phase, orientation, and average crystallite diameter within the seed layers and the overlying $\text{Mg}_3(\text{VO}_4)_2$ films were determined using standard θ - 2θ x-ray diffraction on a Siemens D-500 XRD. The usefulness of this technique is somewhat limited in this experiment because it only probes crystalline planes that are parallel to the substrate. In the case of a highly oriented sample, only one diffraction peak corresponding to a single d-spacing is detectable. This is especially problematic if both the seed layer and the overlying crystalline film are highly oriented and have equal d-spacings, as is the case for our samples. The XRD scans for $\text{Mg}_3(\text{VO}_4)_2$ films deposited onto highly oriented seed layers exhibit only one diffraction peak that could correspond to the seed layer, the overlying $\text{Mg}_3(\text{VO}_4)_2$ film, or both. In order to differentiate between signal generated from each of the two crystalline materials, we performed a more detailed XRD analysis on a Rigaku RTP-300 RC with an area detector collimated down to 100 μm . This XRD configuration enabled us to differentiate the signal generated from each of the thin film materials. Two samples were prepared for this analysis; a 50 nm Au seed layer film deposited at ambient temperature, and an identical Au seed layer with an overlying 200 nm $\text{Mg}_3(\text{VO}_4)_2$ thin film. By comparing the position and relative intensities of the resultant area XRD scans, we were able to verify the crystallinity of the overlying $\text{Mg}_3(\text{VO}_4)_2$ thin film.

Results & Discussion

Deposition of $Mg_3(VO_4)_2$ on Oxidized Si Wafers

$Mg_3(VO_4)_2$ thin films deposited to a thickness of 200 nm onto the amorphous surfaces of oxidized Si wafers are, in effect, amorphous themselves. The XRD scan from such a film deposited at 300 °C fails to exhibit any diffraction peaks corresponding to the thin film as shown in Figure 1. Only the Si (200) and (400) substrate diffraction peaks are visible on the scan. AAS and XPS analyses performed on this sample show a Mg/V atomic ratio of 1.50 ± 0.15 , well within the uncertainty of the measurements, indicating that the films are stoichiometric as deposited.

Crystallinity of Seed Layers

50 nm Ti, Au, Ag and Pt thin film seed layers exhibit strong preferential orientation with the hexagonal close-packed lattice of atoms parallel to the substrates as expected. An XRD scan typical of the four thin film materials deposited onto oxidized Si wafers is shown in Figure 2. Deposition of Ti (300 °C) results in preferential growth in the (0001) (hcp) orientation, while deposition of Pt (300 °C) and Ag (ambient) results in preferential growth along the (111) hcp orientation. Gold thin films deposited at 300 °C show several orientations including (200), (220), (111), and (311). However, deposition of a gold film at ambient temperature results in very strong preferential growth in the (111) hexagonal close-packed orientation as shown in Figure 2.

Deposition of $Mg_3(VO_4)_2$ on Seed Layers

200 nm $\text{Mg}_3(\text{VO}_4)_2$ thin films were deposited onto the four seed layer materials and analyzed using XPS and XRD in order to test for stoichiometry and crystalline structure and orientation. In addition, films of less than 10 nm thickness were also deposited on the titanium and gold seed layers for the reasons given in the Introduction. The seed layer on which the $\text{Mg}_3(\text{VO}_4)_2$ is deposited has a dramatic effect on the properties and behavior of the resultant $\text{Mg}_3(\text{VO}_4)_2$ thin film. $\text{Mg}_3(\text{VO}_4)_2$ thin films deposited onto Ag (111) seed layers at ambient temperature are extremely non-uniform in appearance. XRD scans of these samples show only the Si substrate peaks, suggesting that the $\text{Mg}_3(\text{VO}_4)_2$, Ag, and possibly the Si substrate have reacted to form an amorphous compound. Because of the amorphous nature of the films, deposition of $\text{Mg}_3(\text{VO}_4)_2$ onto Ag (111) was not pursued, and no further analysis was performed.

Deposition of $\text{Mg}_3(\text{VO}_4)_2$ thin films onto well-oriented (0001) Ti thin films results in a highly oriented crystalline structure with the (042) (pseudo-hexagonal) planes parallel to the substrate as indicated by XRD analysis, and the expected Mg/V ratio of 1.5 within experimental error as indicated by XPS analysis. However, deposition and subsequent heating of an 8.5 nm thick $\text{Mg}_3(\text{VO}_4)_2$ film on titanium to 300°C in 50 Torr of oxygen actually results in *reduction* of the V^{5+} to V^{3+} and complete destruction of the $\text{Mg}_3(\text{VO}_4)_2$ structure as evidenced by an increase in the Mg/V XPS ratio to ~3.0. We believe that these results indicate a reaction between the $\text{Mg}_3(\text{VO}_4)_2$ film and the titanium seed layer. Evidently, the affinity of titanium metal for oxygen is so high that it is able to extract oxygen from $\text{Mg}_3(\text{VO}_4)_2$ even under strongly oxidizing conditions, thereby effecting reduction of the vanadium and a disruption of the $\text{Mg}_3(\text{VO}_4)_2$ structure. Although we have achieved the goal of growing a highly oriented, single phase

$\text{Mg}_3(\text{VO}_4)_2$ thin film on Ti (0001), titanium was rejected as a suitable substrate for the growth of ultra-thin, oriented $\text{Mg}_3(\text{VO}_4)_2$ films because of the reactivity between the two film materials.

In contrast to titanium, both gold and platinum have very low affinities for oxygen; neither metal forms an oxide upon heating in air. Thus, seed layers grown from these metals should not suffer from the reactivity problems observed for titanium. Deposition of $\text{Mg}_3(\text{VO}_4)_2$ onto well-oriented (111) Pt thin films resulted in a different orientation of the overlying $\text{Mg}_3(\text{VO}_4)_2$ crystallites. XRD analysis of this sample shows the $\text{Mg}_3(\text{VO}_4)_2$ (312) and possibly the (042) diffraction peaks as shown in Figure 3(a). That there are multiple orientations for the overlying $\text{Mg}_3(\text{VO}_4)_2$ film is not surprising given the significant lattice mismatch (6.9%) between the ions in the $\text{Mg}_3(\text{VO}_4)_2$ (042) and Pt (111) hcp planes.

Deposition of a 200 nm $\text{Mg}_3(\text{VO}_4)_2$ layer onto Au (111) thin films results in $\text{Mg}_3(\text{VO}_4)_2$ thin films that exhibit the most preferential orientation in the desired configuration. Standard θ -2 θ XRD was performed on these samples and the resultant scans show only two peaks; one corresponding to the Au (111)/ $\text{Mg}_3(\text{VO}_4)_2$ (042) planes and one corresponding to the Si (400) substrate as shown in Figure 3(b). This XRD scan is typical for $\text{Mg}_3(\text{VO}_4)_2$ thin deposited onto Au and Ti seed layers. Area XRD analysis also was performed on this sample in order to differentiate the signal resulting from the Au and $\text{Mg}_3(\text{VO}_4)_2$ thin films.

Area XRD scans were collected for an Au (111) seed layer film [Figure 4(a)] and an identically deposited Au (111) seed layer film with a $\text{Mg}_3(\text{VO}_4)_2$ film deposited on top [Figure 4(b)]. The signals were integrated over the same area (i.e. 2 θ range) to enable direct comparisons of the

relative intensities. On Figure 4(a), the very bright arc in the center of the area corresponds to the Au (111) planes that are oriented parallel to the substrate. The lower intensity arc to the left is the $k\beta$ radiation signal from the same set of planes. The very low intensity arc to the right corresponds to a small number of Au (200) planes that are oriented parallel to the substrate. The fact that nearly the entire signal is concentrated along the central Au (111) arc indicates that this Au thin film is very highly oriented with the (111) planes parallel to the substrate. The bright Laue spots correspond to the underlying, single crystal Si substrate. On Figure 4(b), the central arc has a much greater intensity than that of the Au seed layer only shown in Figure 4(a). The substantial increase in signal must result from a contribution from the overlying $Mg_3(VO_4)_2$ thin film. Given the nearly identical d-spacings between the $Mg_3(VO_4)_2$ (042) and the Au (111) sets of planes, $Mg_3(VO_4)_2$ epitaxially grown on the underlying Au seed layer would contribute to the signal in just this manner. The fact that no other diffraction arcs corresponding to $Mg_3(VO_4)_2$ crystallites appear indicates that the $Mg_3(VO_4)_2$ film is either epitaxial or completely amorphous. The increase in signal corresponding to a d-spacing of 2.35 Å indicates that the $Mg_3(VO_4)_2$ (042) planes are responsible for the additional signal. The relative intensities for the Au seed layer (4a) and the Au seed layer with an overlying $Mg_3(VO_4)_2$ film (4b) are plotted in Figure 4(c) for comparison.

XPS analysis of 1, 2, 4, and 200 nm thick $Mg_3(VO_4)_2$ films deposited onto the Au seed layers shows the desired surface stoichiometry in all cases. Furthermore, the films are thermally stable during treatment in vacuum, oxygen, or propane, provided reaction temperatures are kept below 500°C for the 4 and 200 nm films, and 400°C for the 1 and 2 nm films. Further details on the effects of reactive treatments will be given in a forthcoming paper [11], but one result is of

particular interest here. Wang *et al.* [12] showed that $\text{Mg}_3(\text{VO}_4)_2$ powders undergo a transformation to cubic spinel $\text{Mg}_3\text{V}_2\text{O}_6$ during high temperature reduction in hydrogen. This transformation occurs by a topochemical reaction which leaves the psuedo-hcp arrangement of the oxygen atoms unchanged but alters the locations of the Mg and V cations. We have reproduced this experiment on the 200 nm $\text{Mg}_3(\text{VO}_4)_2$ on Au (111) film by treating the film in 100 Torr propane for 1 h at 500 °C. XPS shows complete reduction of V^{5+} to V^{3+} and XRD of the reduced film shows (111), (222), and (444) peaks of $\text{Mg}_3\text{V}_2\text{O}_6$ (Figure 5) exactly as expected for topochemical conversion of an (042) oriented $\text{Mg}_3(\text{VO}_4)_2$ film into a (111) oriented $\text{Mg}_3\text{V}_2\text{O}_6$ film. This result not only supports the conclusion that the desired orientation of the $\text{Mg}_3(\text{VO}_4)_2$ film has been achieved, but also demonstrates that the films behave very much like bulk $\text{Mg}_3(\text{VO}_4)_2$ powders, and are therefore excellent model catalysts. The Au (200) and (220) diffraction peaks (Figure 5) are usually detectable using XRD following a thermal or reactive treatment of the samples. However, their intensity is always orders of magnitude lower than that of the Au (111)/ $\text{Mg}_3(\text{VO}_4)_2$ (042) diffraction peak. Therefore, their presence does not indicate significant reconstruction of the Au seed layer film. Thus, it appears that the Au (111) seed layer is the most desirable from the standpoint of obtaining highly oriented, ultra-thin, stable films of $\text{Mg}_3(\text{VO}_4)_2$ with chemical properties similar to bulk $\text{Mg}_3(\text{VO}_4)_2$ powders.

Conclusions

We have successfully grown stoichiometric $\text{Mg}_3(\text{VO}_4)_2$ thin films oriented with the hexagonal (042) plane parallel to the substrate on a variety of conducting seed layers including Au (111), Ag (111), Pt (111), and Ti (0001). Based on the criteria of thermal stability and orientational order, Au (111) is the most desirable substrate material. Au does not react with $\text{Mg}_3(\text{VO}_4)_2$ and

the films show excellent preferential (042) orientation. Furthermore, the films display chemical reduction behavior that closely resembles the behavior of bulk $\text{Mg}_3(\text{VO}_4)_2$ powders, indicating that these thin films are excellent models for bulk catalytic materials. We have determined that the ultrathin films do indeed minimize or eliminate charging effects typically encountered during electron and ion spectroscopy studies of oxides [11]. The behavior of ultrathin $\text{Mg}_3(\text{VO}_4)_2$ films on Au (111) during treatments in reactive environments typically encountered during oxidative dehydrogenation of small alkanes is presently under investigation.

Acknowledgements

We gratefully acknowledge Dr. John A. Shelnett for his assistance in modeling the $\text{Mg}_3(\text{VO}_4)_2$ crystal structure.

Material	Crystal structure	hcp plane	Spacing in hcp plane (Å)	Lattice mismatch with $\text{Mg}_3(\text{VO}_4)_2$ (%)
Ti	hcp	(0002)	2.95	0.3
Ag	fcc	(111)	2.86	2.4
Au	fcc	(111)	2.88	2.8
Pt	fcc	(111)	2.77	6.9

Table I: Candidate “seed” layer materials for inducing epitaxial growth of $\text{Mg}_3(\text{VO}_4)_2$ (042).

Thin Film Material	Temperature (°C)	Ar flow (sccm)	O ₂ flow (sccm)	Power (W)	Dep. Rate (nm/min)	Thickness (nm)
Ti	300	75	0	77 (DC)	5.9	50
Ag	Ambient	75	0	2.4 (DC)	7.7	50
Au	Ambient	75	0	4.3 (DC)	8.8	50
Au	300	75	0	4.3 (DC)	8.8	50
Pt	300	75	0	5.8 (DC)	7.2	50
Mg ₃ (VO ₄) ₂	300	75	2.5	241 (RF)	6.4	Varied

Table II Deposition parameters for Mg₃(VO₄)₂ thin films and various metal seed layers.

Figure Captions

Figure 1 XRD scan of an $\text{Mg}_3(\text{VO}_4)_2$ film deposited onto an oxidized Si wafer. Only substrate diffraction peaks are visible, indicating that the overlying $\text{Mg}_3(\text{VO}_4)_2$ film is amorphous.

Figure 2 XRD scan of an Au film deposited at ambient temperature onto an oxidized Si wafer. Only the substrate and Au (111) diffraction peaks are visible, indicating a highly oriented Au thin film. Similar XRD scans are obtained for the other seed layer materials.

Figure 3(a) XRD scan of a 200 nm $\text{Mg}_3(\text{VO}_4)_2$ film deposited on a Pt seed layer at 300 °C. Several $\text{Mg}_3(\text{VO}_4)_2$ peaks are visible indicating that $\text{Mg}_3(\text{VO}_4)_2$ is crystalline but randomly oriented.

Figure 3(b) XRD scan of a 200 nm $\text{Mg}_3(\text{VO}_4)_2$ film deposited on an Au seed layer at 300 °C. Only the substrate and Au (111)/ $\text{Mg}_3(\text{VO}_4)_2$ (042) diffraction peaks are visible, indicating that the Au and possibly the $\text{Mg}_3(\text{VO}_4)_2$ are highly oriented.

Figure 4(a) Area XRD scan of an Au seed layer deposited at ambient temperature. The bright arc in the center corresponds to the Au (111) set of planes parallel to the substrate.

Figure 4(b) Area XRD scan of an identically deposited Au seed layer with an overlying 200 nm $\text{Mg}_3(\text{VO}_4)_2$ thin film. The increase in signal of the central arc indicates that the $\text{Mg}_3(\text{VO}_4)_2$ is contributing to the intensity for the corresponding d-spacing (2.35 Å) and consequently must be preferentially oriented parallel to the substrate.

Figure 4(c) Integrated intensities of area XRD scans shown in (a) and (b).

Figure 5 XRD scan of a film deposited as $\text{Mg}_3(\text{VO}_4)_2$ onto an Au seed layer and then reduced for 1h at 500°C in 100 Torr propane. The resultant scan shows several $\text{Mg}_3\text{V}_2\text{O}_6$ (reduced) diffraction peaks from the (111) planes.

Figure 1

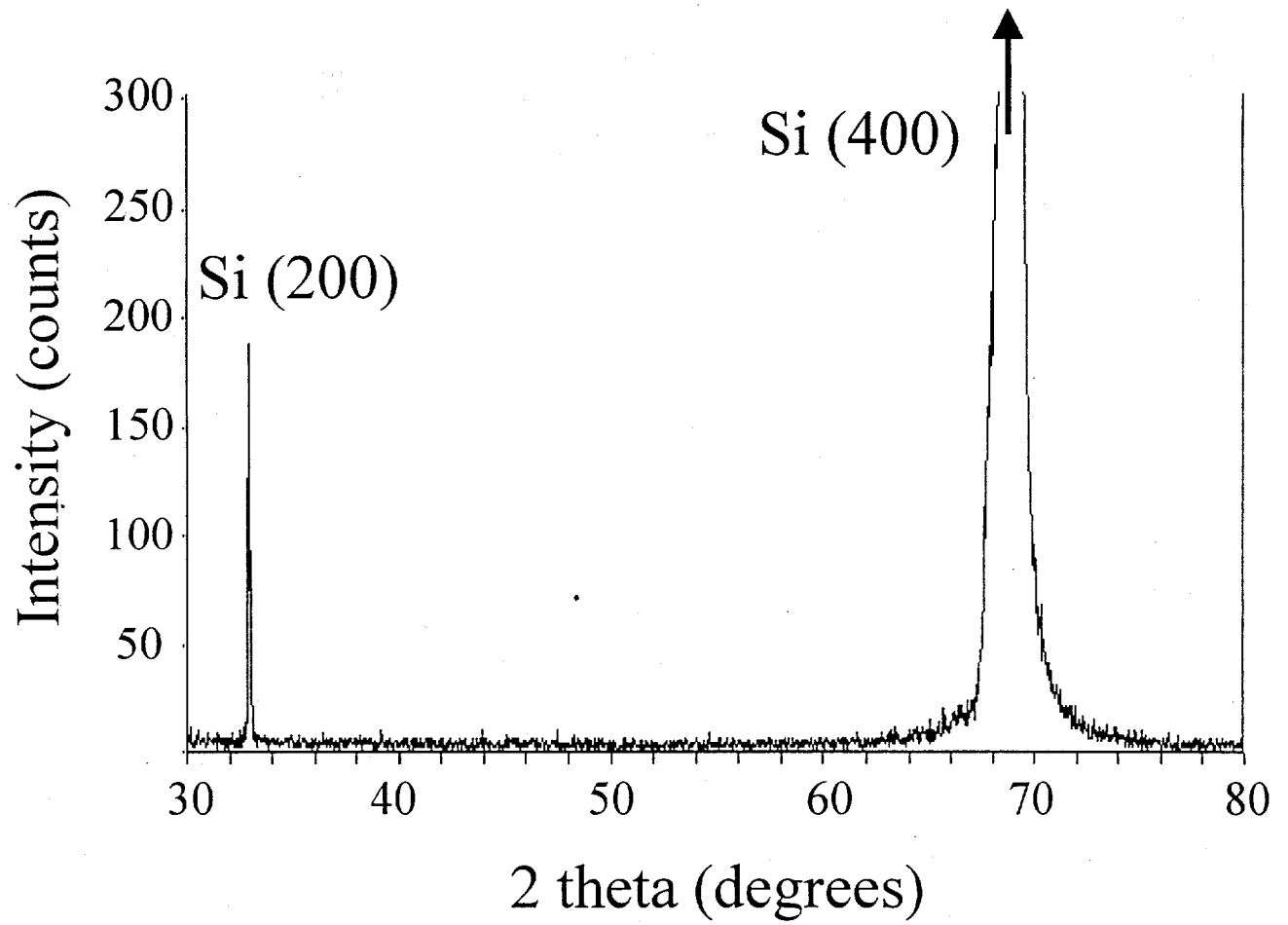


Figure 2

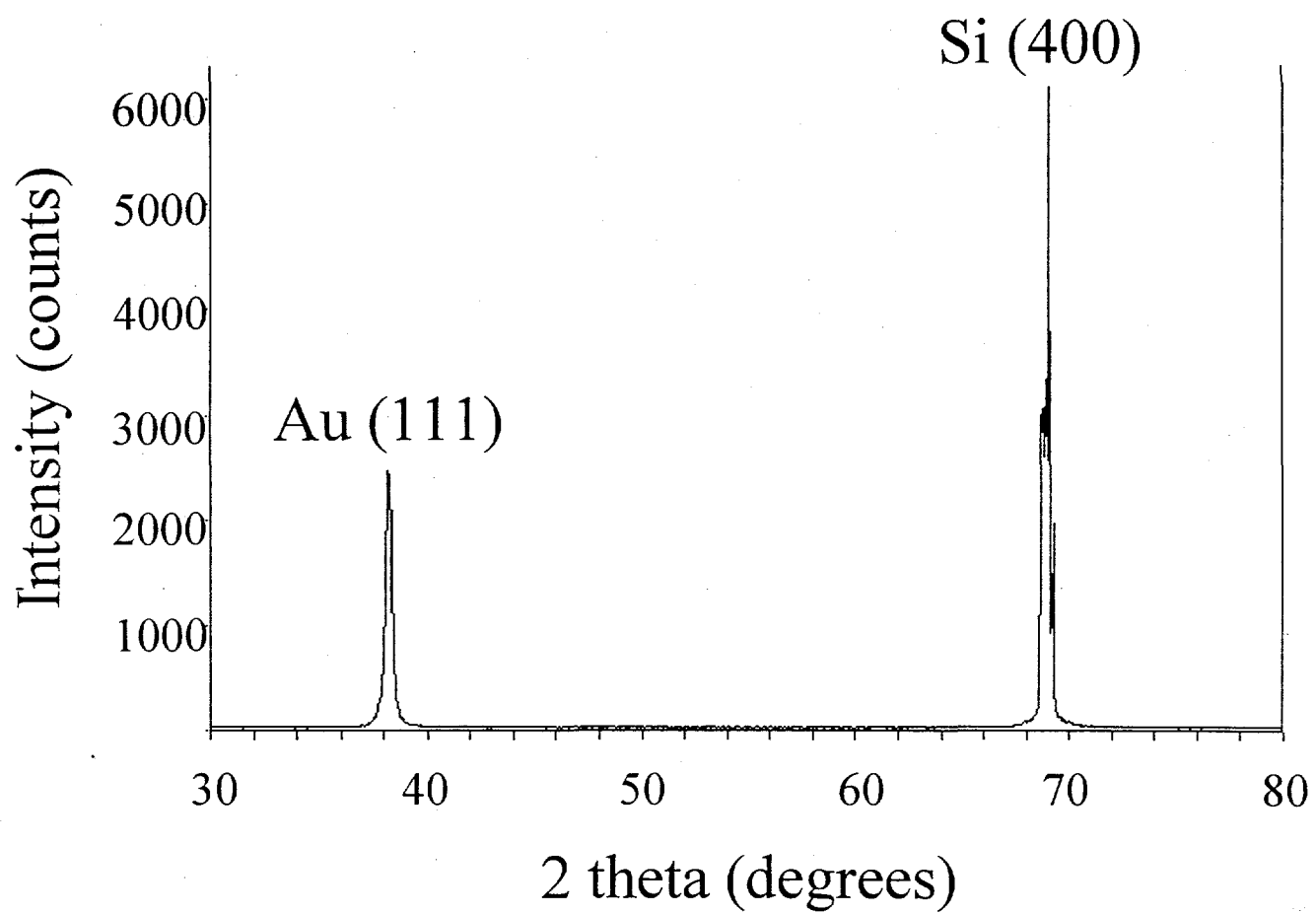


Figure 3(a)

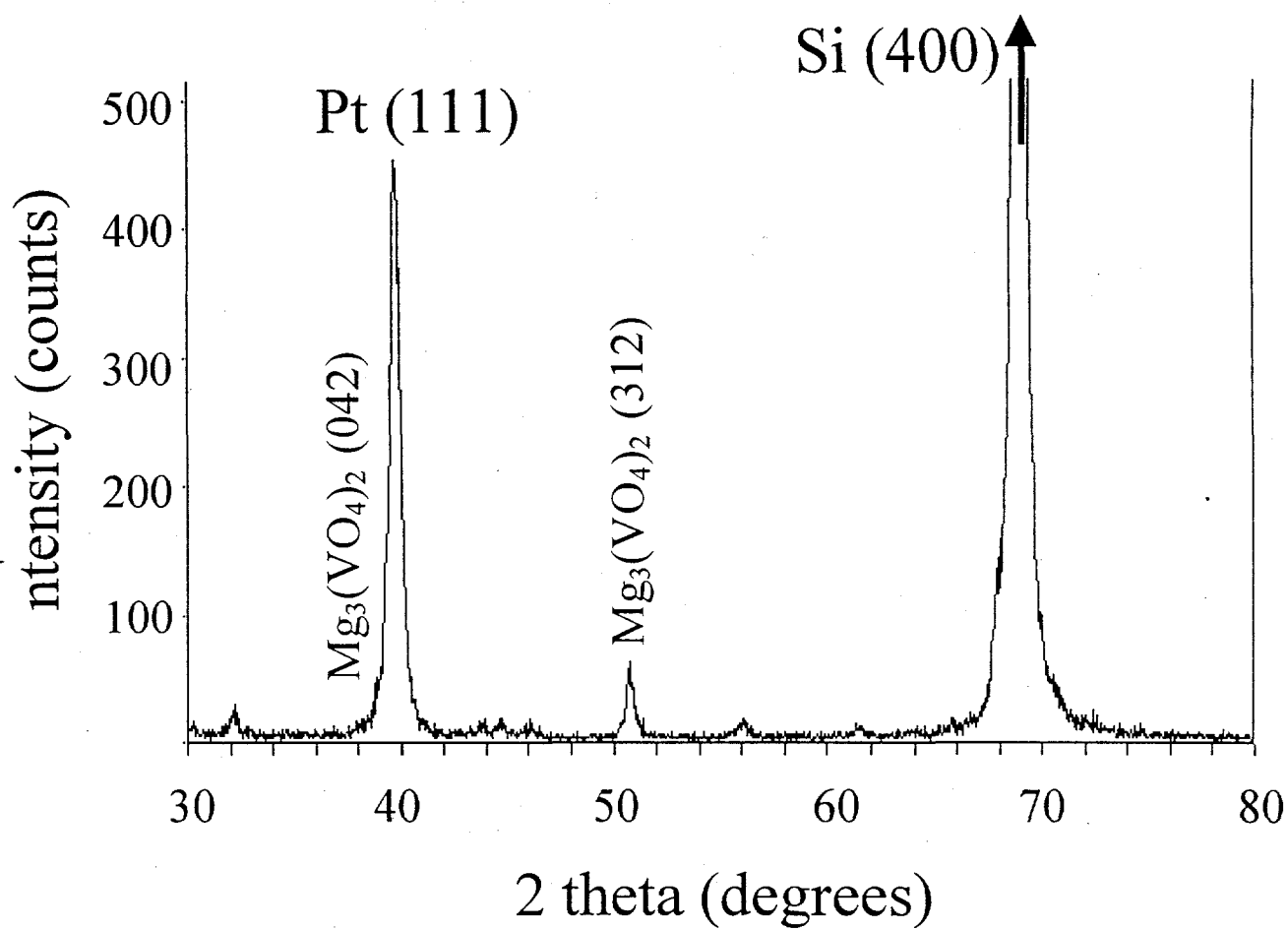


Figure 3(b)

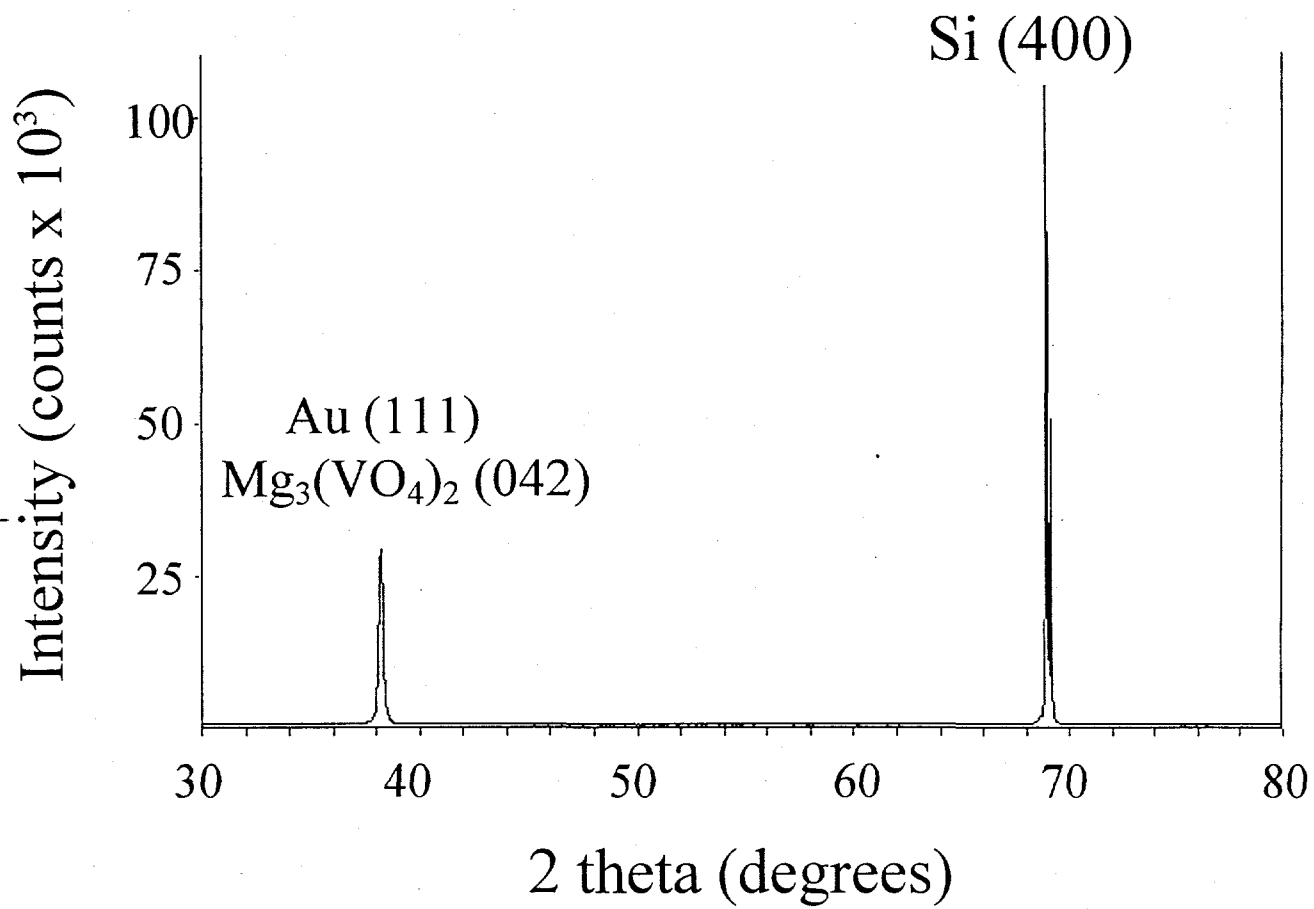


Figure 4(a) ann 4(b)

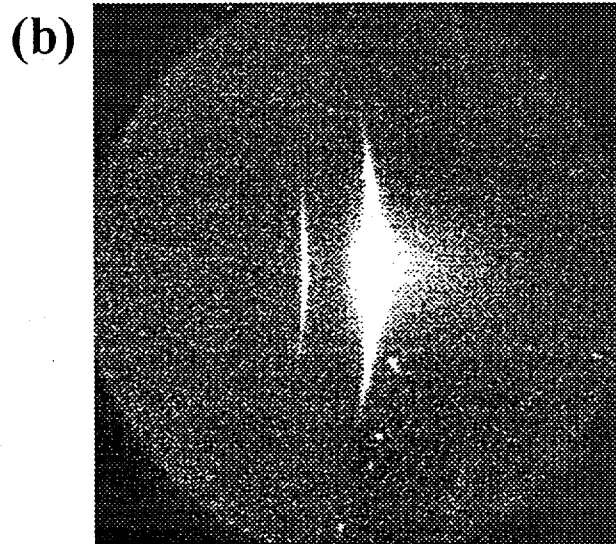
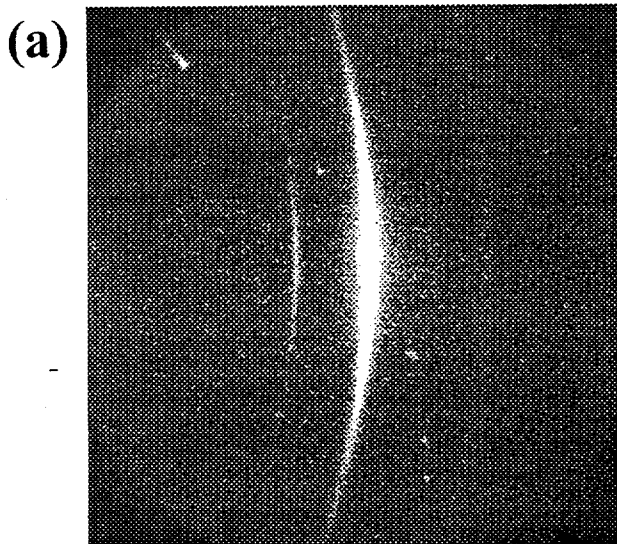


Figure 4(c)

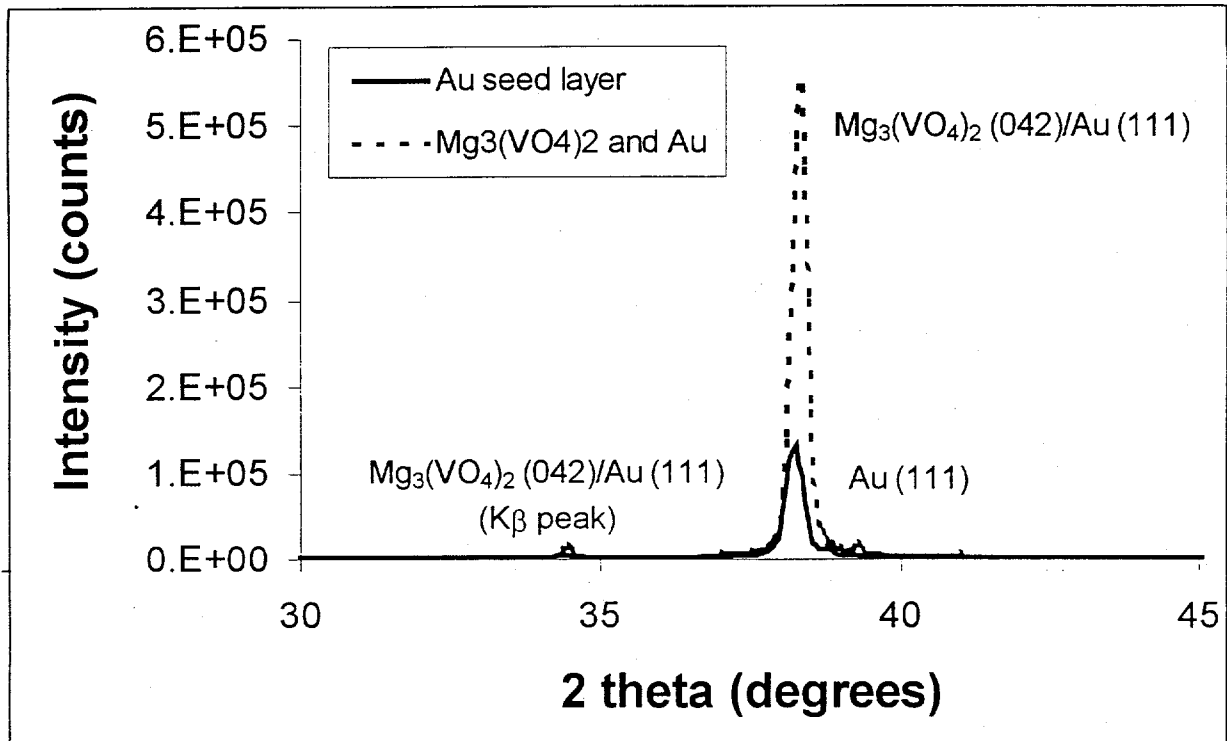
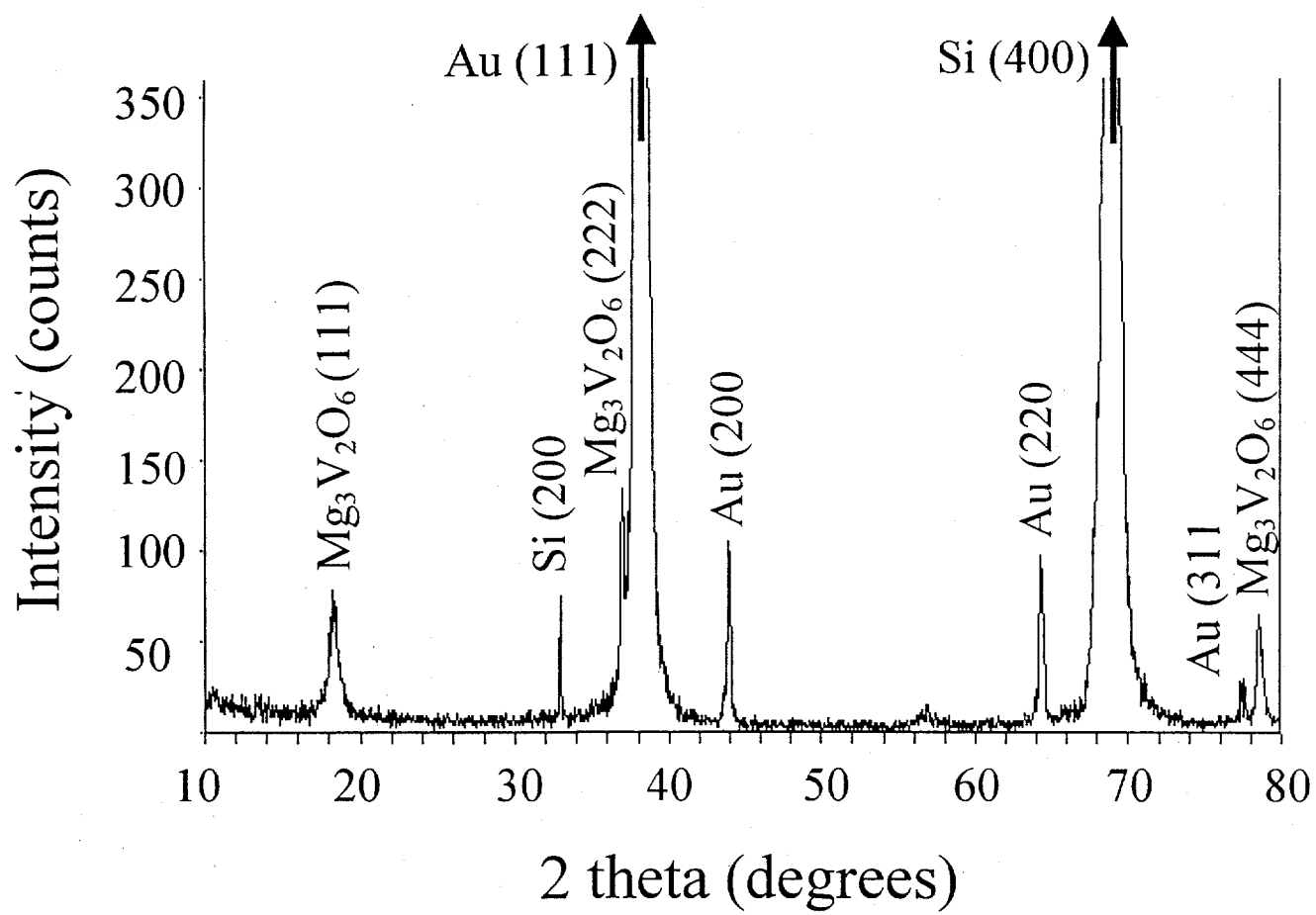


Figure 5



References

- 1 H. H. Kung in "Advances in Catalysis," Vol. 40, (W. O. Haag, Ed.), Academic Press, Inc. (1991) p. 1.
- 2 M. A. Char, D. Patel and H. H. Kung, *J. Catal.* **109**, (1988) p. 463.
- 3 K. Seshan, H. M. Swann, R. H. H. Smits, J. G. van Ommen and J. R. H. Ross in "New Developments in Selective Oxidation" (G. Centi and F. Trifiro, Eds.) Elsevier Press, Amsterdam, (1990), p. 505.
- 4 J. Libuda, F. Winkelmann, M. Baumer, H.-J. Freund, Th. Bertrams, H. Neddermeyer, and K. Muller, *Surface Sci.* **318**, (1994) p. 61.
- 5 D. R. Rainer, C. Xu, and D. W. Goodman, *J. Molec. Catal.* **A119**, (1997) p. 307.
- 6 PDF card 19-0778, JCPDS – International Center for Diffraction Data, Newtown Square, PA.
- 7 PDF card 37-0351, JCPDS – International Center for Diffraction Data, Newtown Square, PA.
- 8 D. S. H. Sam, V. Soenen, and J. C. Volta, *J. Catalysis* **123**, (1990) p. 417.
- 9 N. Krishnamachari and C. Calvo, *Can. J. Chem.* **49**, (1971) p. 1629.
- 10 C. D. Wagner, L. E. Davis, M. V. Zoeller, J. A. Taylor, R. M. Raymond, and L. H. Gale, *Surf. Interface Anal.* **3**, (1981) p. 211.
- 11 A. G. Sault and J. A. Ruffner, to be published, 1999.
- 12 X. Wang, H. Zhang, W. Sinkler, K. R. Poppelmeier, and L. D. Marks, *J. Alloys and Compounds* **270**, (1998) p. 88.